Supplement of Atmos. Chem. Phys., 24, 2861–2883, 2024
https://doi.org/10.5194/acp-24-2861-2024-supplement


Atmospheric Chemistry and Physics
Open Access

*Supplement of*

# A remote sensing algorithm for vertically resolved cloud condensation nuclei number concentrations from airborne and spaceborne lidar observations

**Piyushkumar N. Patel et al.**

*Correspondence to:* Piyushkumar N. Patel (piyushether@gmail.com, piyushkumar.n.patel@jpl.nasa.gov)

# <u>Supplementary Information</u>

Table S1: Typical range of lidar-derived depolarization ratios of dust and non-dust (pollution and marine) components. These values are compiled from various field campaign, cruise measurements, data from PollyNET/EARLINET stations. In our study, we use the average values of these ranges to distinguish dust and non-dust component within the dust mixture.

| Parameters | 355 nm | 532 nm | 1064 nm | References |
|---|---|---|---|---|
| | | Dust | | |
| Depolarization ratio | 0.22 – 0.26 | 0.27 – 0.35 | 0.03 – 0.1 | (Preißler et al., 2011; Groß et al., 2011; Kanitz et al., 2013; Baars et al., 2016; Haarig et al., 2017; Bohlmann et al., 2018; Haarig et al., 2022; Rittmeister et al., 2017; Kaduk, 2017; Szczepanik et al., 2021; Hofer et al., 2020; Müller et al., 2007; Filioglou et al., 2020) |
| | | Non-dust | | |
| Depolarization ratio | 0.02 – 0.09 | 0.02 – 0.05 | 0.01 – 0.04 | (Ansmann et al., 2005; Müller et al., 2007; Tesche et al., 2007; Komppula et al., 2012; Preißler et al., 2013; Hänel et al., 2012; Giannakaki et al., 2016; Heese et al., 2017; Kaduk, 2017; Janicka et al., 2016; Rittmeister et al., 2017; Gasteiger et al., 2011; Bohlmann et al., 2018) |

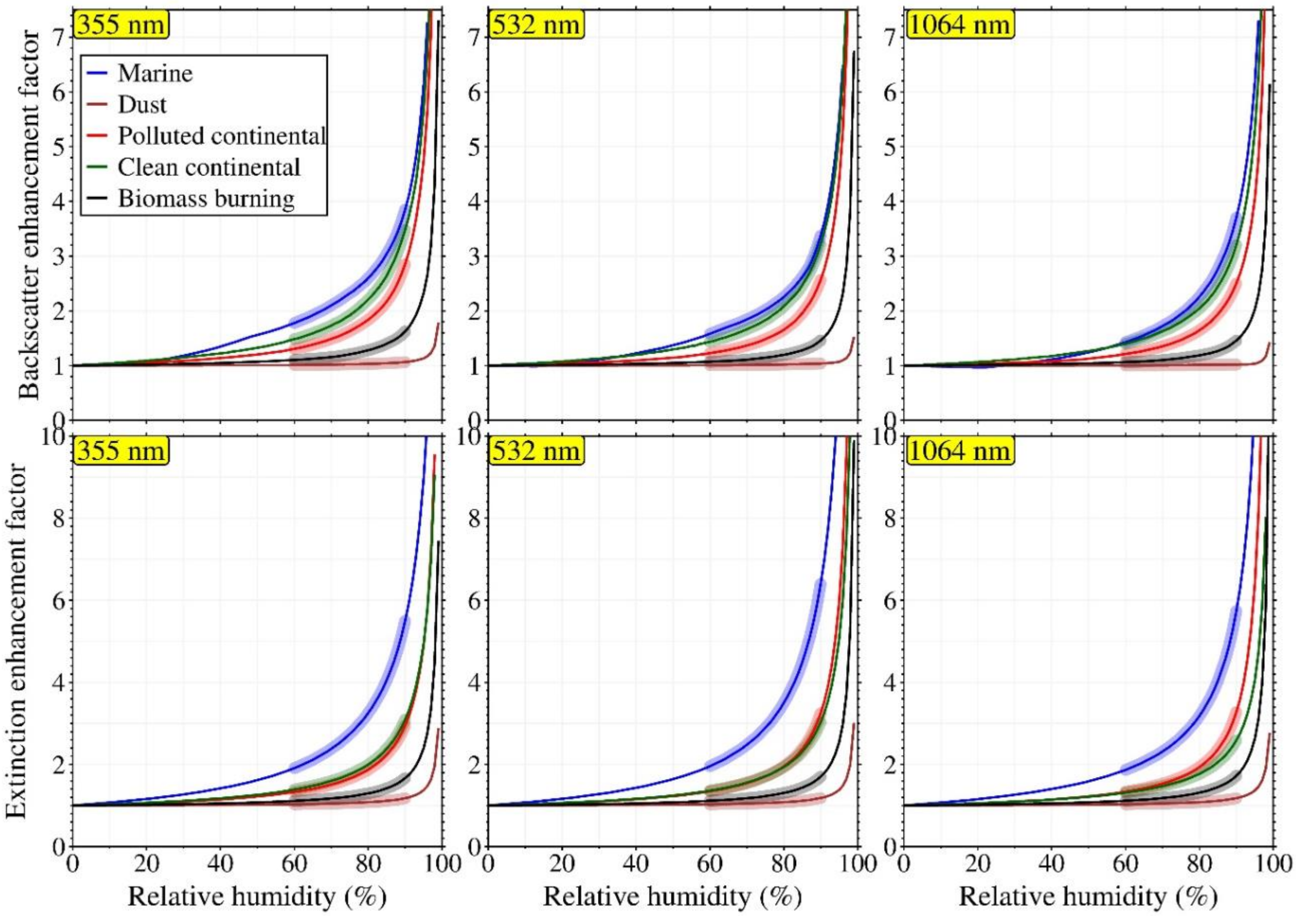


Figure S1: Mean enhancement factor for backscatter and extinction coefficients at 355, 532 and 1064 nm are fitted using Eq (6) for five aerosol subtypes. This mean fitting curve is calculated with the set of PNSD and κ considered for the construction of LUTs. The thin line represents Mie model simulations, and the highlighted thick line (within RH range of 60-90%) are used to fit parameterization lines.

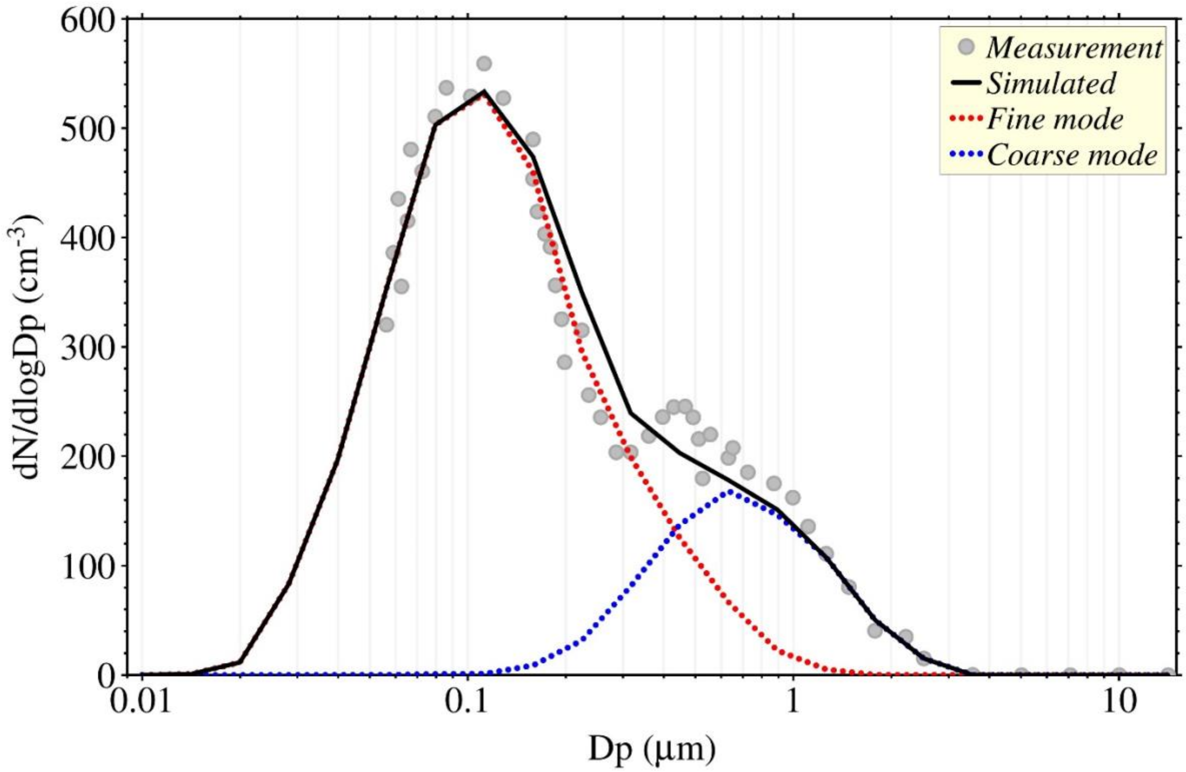


Figure S2: Observed aerosol particle size distribution during the NASA Oracles mission. Particle size is represented by the geometric diameter. Solid dots denote integrated Ultra-High Sensitivity Aerosol Spectrometer (UHSAS) and Aerodynamic Particle Sizer (APS) measurements. Curves are bimodal lognormal fits for the size distributions of the fine mode (red dotted line), the coarse mode (blue dotted line), and the full mode (black solid line).

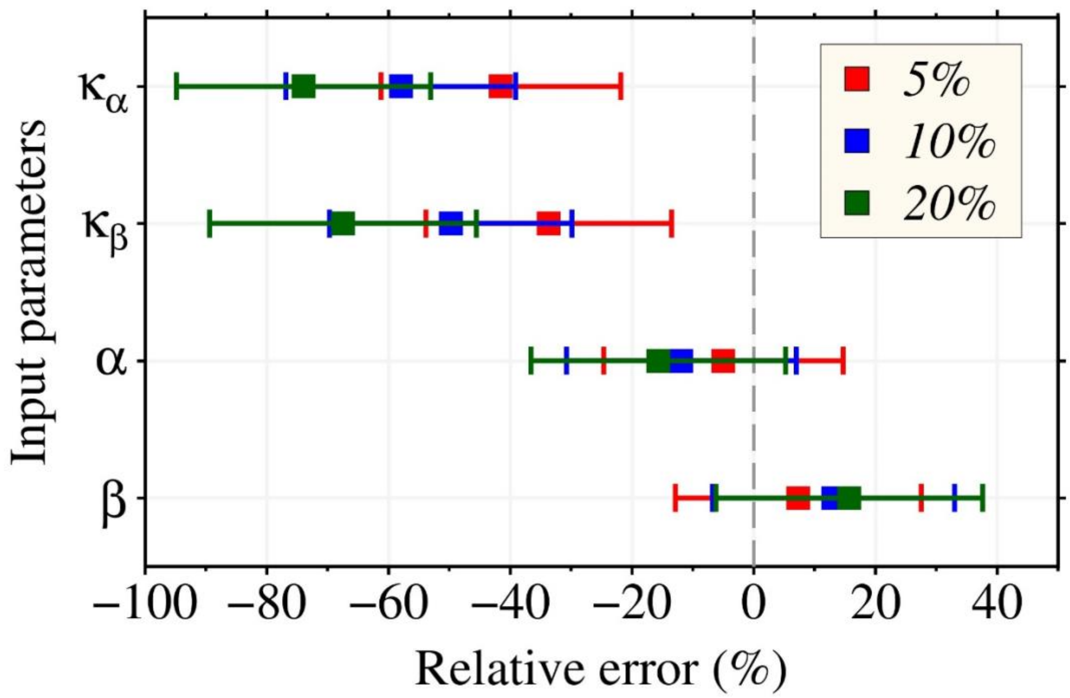


Figure S3: Relative errors in input parameters (backscattering coefficient, extinction coefficient, enhancement factor of backscatter coefficients and enhancement factor of extinction coefficients) with 5%, 10% and 20% of random error in relative humidity (RH). The dots are the median values and the error bars denote the 5th and 95th percentile.

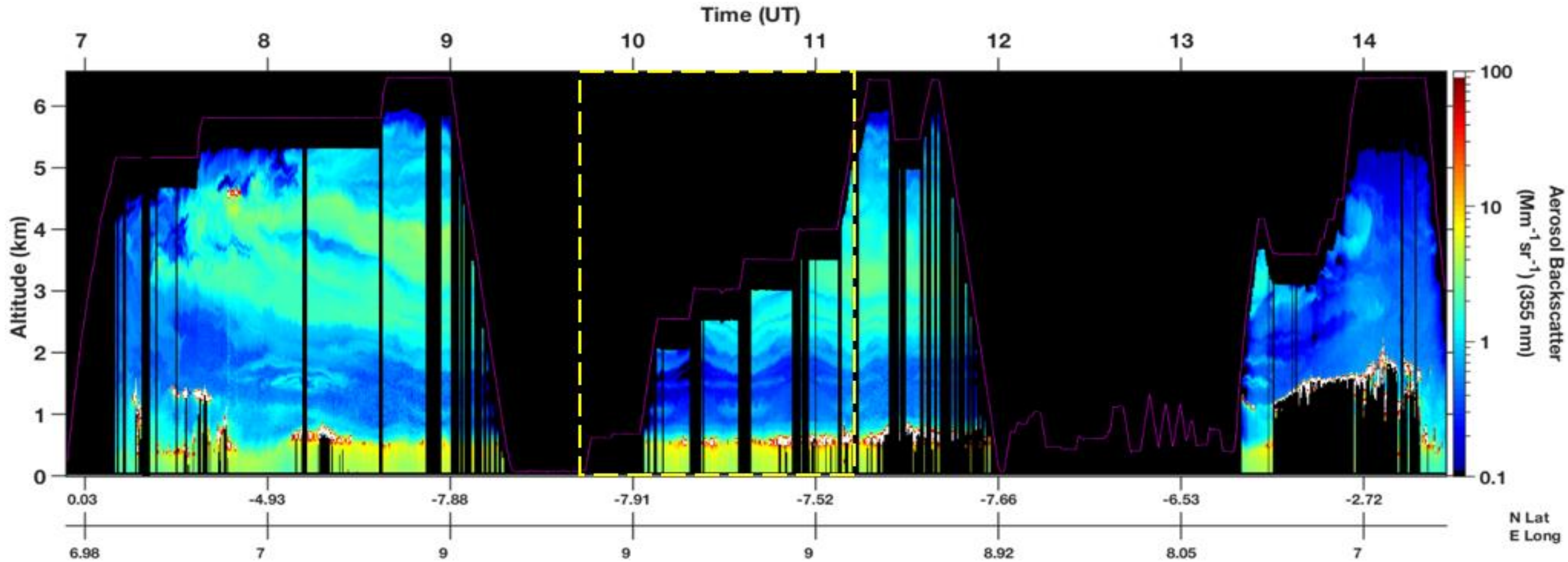


Figure S4: The HSRL-2 derived aerosol backscatter at 355 nm from the flight of NASA ORACLES campaign on 19 October 2018. The pink line displays the flight trajectory, whereas the yellow dotted line box illustrates the region of interest with the ascending of flight were used for the profile-based validation of ECLiAP retrieved NCCN from HSRL-2 measurements against the measured NCCN from CCN counter.

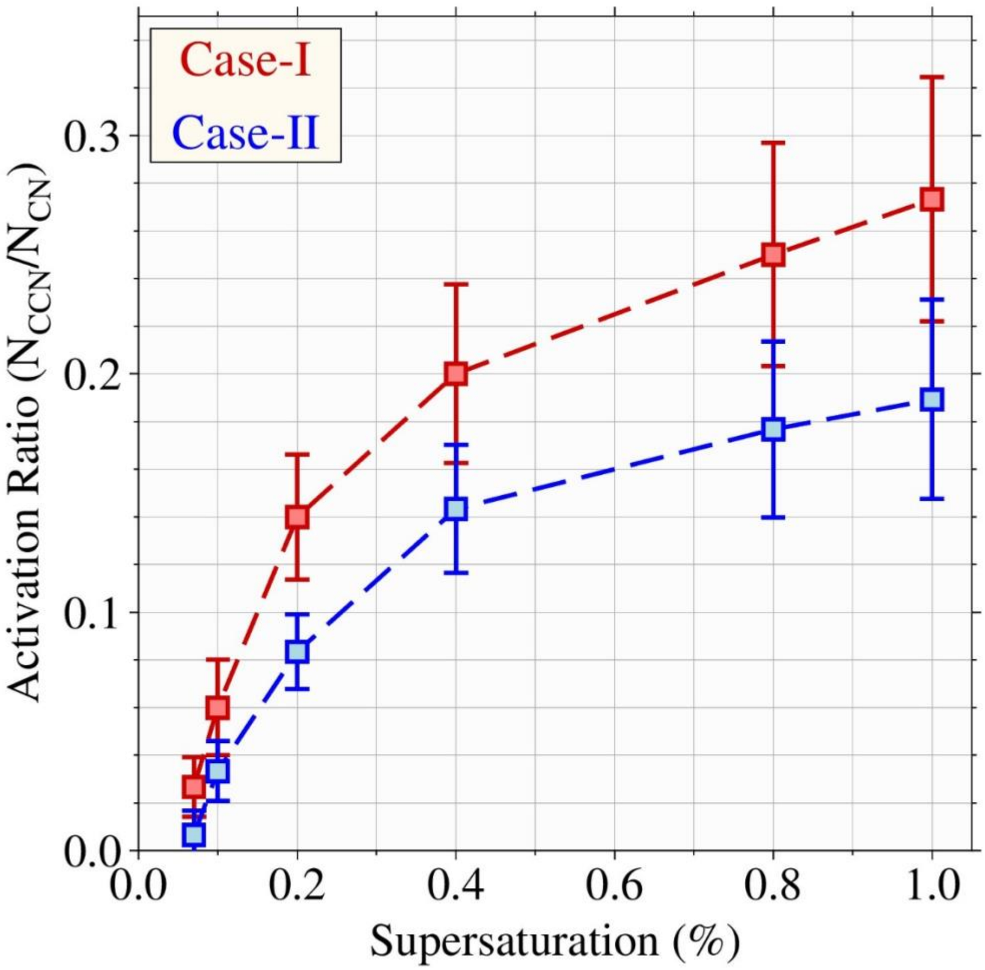


Figure S5: The mean activation ratio spectra as a function of supersaturation for the case-I and case-II identified from the CALIOP observations on 01 January 2019.

Ansmann, A., Engelmann, R., Althausen, D., Wandinger, U., Hu, M., Zhang, Y., and He, Q.: High aerosol load over the Pearl River Delta, China, observed with Raman lidar and Sun photometer, Geophys. Res. Lett., 32, 1–4, https://doi.org/10.1029/2005GL023094, 2005.

Baars, H., Kanitz, T., Engelmann, R., Althausen, D., Heese, B., Komppula, M., Preißler, J., Tesche, M., Ansmann, A., Wandinger, U., Lim, J. H., Young Ahn, J., Stachlewska, I. S., Amiridis, V., Marinou, E., Seifert, P., Hofer, J., Skupin, A., Schneider, F., Bohlmann, S., Foth, A., Bley, S., Pfüller, A., Giannakaki, E., Lihavainen, H., Viisanen, Y., Kumar Hooda, R., Pereira, S. N., Bortoli, D., Wagner, F., Mattis, I., Janicka, L., Markowicz, K. M., Achtert, P., Artaxo, P., Pauliquevis, T., Souza, R. A. F., Prakesh Sharma, V., Gideon Van Zyl, P., Paul Beukes, J., Sun, J., Rohwer, E. G., Deng, R., Mamouri, R. E., and Zamorano, F.: An overview of the first decade of PollyNET: An emerging network of automated Raman-polarization lidars for continuous aerosol profiling, Atmos. Chem. Phys., 16, 5111–5137, https://doi.org/10.5194/ACP-16-5111-2016, 2016.

Bohlmann, S., Baars, H., Radenz, M., Engelmann, R., and Macke, A.: Ship-borne aerosol profiling with lidar over the Atlantic Ocean: From pure marine conditions to complex dust-smoke mixtures, Atmos. Chem. Phys., 18, 9661–9679, https://doi.org/10.5194/ACP-18-9661-2018, 2018.

Filioglou, M., Giannakaki, E., Backman, J., Kesti, J., Hirsikko, A., Engelmann, R., O'Connor, E., Leskinen, J. T. T., Shang, X., Korhonen, H., Lihavainen, H., Romakkaniemi, S., and Komppula, M.: Optical and geometrical aerosol particle properties over the United Arab Emirates, Atmos. Chem. Phys., 20, 8909–8922, https://doi.org/10.5194/ACP-20-8909-2020, 2020.

Gasteiger, J., Grobß, S., Freudenthaler, V., and Wiegner, M.: Volcanic ash from Iceland over Munich: Mass concentration retrieved from ground-based remote sensing measurements, Atmos. Chem. Phys., 11, 2209–2223, https://doi.org/10.5194/ACP-11-2209-2011, 2011.

Giannakaki, E., Van Zyl, P. G., Müller, D., Balis, D., and Komppula, M.: Optical and microphysical characterization of aerosol layers over South Africa by means of multi-wavelength depolarization and Raman lidar measurements, Atmos. Chem. Phys., 16, 8109–8123, https://doi.org/10.5194/ACP-16-8109-2016, 2016.

Groß, S., Tesche, M., Freudenthaler, V., Toledano, C., Wiegner, M., Ansmann, A., Althausen, D., and Seefeldner, M.: Characterization of Saharan dust, marine aerosols and mixtures of biomass-burning aerosols and dust by means of multi-wavelength depolarization and Raman lidar measurements during SAMUM 2, Tellus B Chem Phys Meteorol, 63, 706–724, https://doi.org/10.1111/J.1600-0889.2011.00556.X, 2011.

Haarig, M., Ansmann, A., Althausen, D., Klepel, A., Groß, S., Freudenthaler, V., Toledano, C., Mamouri, R. E., Farrell, D. A., Prescod, D. A., Marinou, E., Burton, S. P., Gasteiger, J., Engelmann, R., and Baars, H.: Triple-wavelength depolarization-ratio profiling of Saharan dust over Barbados during SALTRACE in 2013 and 2014, Atmos. Chem. Phys., 17, 10767–10794, https://doi.org/10.5194/ACP-17-10767-2017, 2017.

Haarig, M., Ansmann, A., Engelmann, R., Baars, H., Toledano, C., Torres, B., Althausen, D., Radenz, M., and Wandinger, U.: First triple-wavelength lidar observations of depolarization and extinction-to-backscatter ratios of Saharan dust, Atmos. Chem. Phys., 22, 355–369, https://doi.org/10.5194/ACP-22-355-2022, 2022.

Hänel, A., Baars, H., Althausen, D., Ansmann, A., Engelmann, R., and Sun, J. Y.: One-year aerosol profiling with EUCAARI Raman lidar at Shangdianzi GAW station: Beijing plume and seasonal variations, J. Geophys. Res. Atmos., 117, https://doi.org/10.1029/2012JD017577, 2012.

Heese, B., Baars, H., Bohlmann, S., Althausen, D., and Deng, R.: Continuous vertical aerosol profiling with a multi-wavelength Raman polarization lidar over the Pearl River Delta, China, Atmos. Chem. Phys., 17, 6679–6691, https://doi.org/10.5194/ACP-17-6679-2017, 2017.

Hofer, J., Ansmann, A., Althausen, D., Engelmann, R., Baars, H., Wadinga Fomba, K., Wandinger, U., Abdullaev, S. F., and Makhmudov, A. N.: Optical properties of Central Asian aerosol relevant for spaceborne lidar applications and aerosol typing at 355 and 532nm, Atmos. Chem. Phys.,, 20, 9265–9280, https://doi.org/10.5194/ACP-20-9265-2020, 2020.

Janicka, L., Stachlewska, I. S., Markowicz, K. M., Baars, H., Engelmann, R., and Heese, B.: Lidar Measurements of Canadian Forest Fire Smoke Episode Observed in July 2013 over Warsaw, Poland, EPJ Web Conf, 119, https://doi.org/10.1051/EPJCONF/201611918005, 2016.

Kaduk, C.: Characterization of the optical properties of complex aerosol mixtures observed with a multiwavelength–Raman– polarization lidar during the 6-weeks BACCHUS campaign in Cyprus in spring 2015, Leipzig University, 2017.

Kanitz, T., Ansmann, A., Engelmann, R., and Althausen, D.: North-south cross sections of the vertical aerosol distribution over the Atlantic Ocean from multiwavelength Raman/polarization lidar during Polarstern cruises, J. Geophys. Res. Atmos., 118, 2643–2655, https://doi.org/10.1002/JGRD.50273, 2013.

Komppula, M., Mielonen, T., Arola, A., Korhonen, K., Lihavainen, H., Hyv̈arinen, A. P., Baars, H., Engelmann, R., Althausen, D., Ansmann, A., Müller, D., Panwar, T. S., Hooda, R. K., Sharma, V. P., Kerminen, V. M., Lehtinen, K. E. J., and Viisanen, Y.: Technical Note: One year of Raman-lidar measurements in Gual Pahari EUCAARI site close to New Delhi in India-Seasonal characteristics of the aerosol vertical structure, Atmos. Chem. Phys., 12, 4513–4524, https://doi.org/10.5194/ACP-12-4513-2012, 2012.

Müller, D., Ansmann, A., Mattis, I., Tesche, M., Wandinger, U., Althausen, D., and Pisani, G.: Aerosol-type-dependent lidar ratios observed with Raman lidar, J. Geophys. Res. Atmos., 112, https://doi.org/10.1029/2006JD008292, 2007.

Preißler, J., Wagner, F., Pereira, S. N., and Guerrero-Rascado, J. L.: Multi-instrumental observation of an exceptionally strong Saharan dust outbreak over Portugal, J. Geophys. Res. Atmos., 116, https://doi.org/10.1029/2011JD016527, 2011.

Preißler, J., Wagner, F., Guerrero-Rascado, J. L., and Silva, A. M.: Two years of free-tropospheric aerosol layers observed over Portugal by lidar, J. Geophys. Res. Atmos., 118, 3676–3686, https://doi.org/10.1002/JGRD.50350, 2013.

Rittmeister, F., Ansmann, A., Engelmann, R., Skupin, A., Baars, H., Kanitz, T., and Kinne, S.: Profiling of Saharan dust from the Caribbean to western Africa-Part 1: Layering structures and optical properties from shipborne polarization/Raman lidar observations, Atmos. Chem. Phys., 17, 12963–12983, https://doi.org/10.5194/ACP-17-12963-2017, 2017.

Szczepanik, D. M., Stachlewska, I. S., Tetoni, E., and Althausen, D.: Properties of Saharan Dust Versus Local Urban Dust—A Case Study, Earth Space Sci., 8, https://doi.org/10.1029/2021EA001816, 2021.

Tesche, M., Ansmann, A., Müller, D., Althausen, D., Engelmann, R., Hu, M., and Zhang, Y.: Particle backscatter, extinction, and lidar ratio profiling with Raman lidar in south and north China, Appl. Opt., 46, 6302–6308, https://doi.org/10.1364/AO.46.006302, 2007.